JOURNAL OF GEOPHYSICAL RESEARCH, VOL. 103, NO. D5, PAGES 5707–5717, MARCH 20, 1998

Photochemical alkene formation in seawater from dissolved organic carbon: Results from laboratory experiments

M. Ratte and O. Bujok[1]
Institut für Atmosphärische Chemie, Jülich, Germany

A. Spitzy
Institut für Biogeochemie und Meereschemie, Universität Hamburg, Hamburg, Germany

J. Rudolph[2]
Institut fur Atmospharische Chemie, Jülich, Germany

Abstract. The production mechanism of light alkenes, alkanes, and isoprene was investigated in laboratory experiments by measuring their concentrations in natural seawater as a function of spectral range, exposure time and origin, and concentration of dissolved organic carbon (DOC). The production mechanism of alkanes and of isoprene could not be clarified. Ethene and propene are produced photochemically from DOC. The relevant spectral range is UV and short-wavelength visible light. Initial production rates (up to day 10 of exposure) were in the range of several pmol L^{-1} h^{-1} (mg DOC)$^{-1}$; the corresponding mean quantum yields for the spectral range of 300–420 nm were about 10^{-8}. Generally, the production rates and the quantum yields for ethene were about 2 times that of propene. The key factors in the total column integrated oceanic alkene production are the solar photon flux at sea surface, the penetration depth of the light into the ocean (especially the relation between different light absorbers, i.e., the extinction due to absorption of DOC), and the wavelength- and DOC-dependent quantum yields. As a result of the high variability of these parameters, actual local alkene production rates for a specific oceanic region may differ considerably from the globally averaged oceanic alkene production rates. The latter were estimated to be at most 5 Mt yr^{-1}.

1. Introduction

Oceanic dissolved organic carbon (DOC) represents one of the largest organic carbon reservoirs on Earth [*Druffel et al.*, 1992]. Due to its photochemical degradation by sunlight, a large number of biologically labile and volatile organic compounds can be formed [*Ferek and Andreae*, 1984; *Kieber et al.*, 1989, 1990; *Mopper et al.*, 1991; *Moore and Zafiriou*, 1994; *Weiss et al.*, 1995; *Zuo and Jones*, 1995]. *Wilson et al.* [1970] were the first to publish experimental results pointing to photochemical production of unsaturated hydrocarbons in seawater from DOC. Alkenes may substantially affect local tropospheric chemistry, and due to their high reactivity and thus short lifetime their dominant source in the remote marine troposphere is emissions from seawater [*Rudolph and Ehhalt*, 1981; *Bonsang et al.*, 1988; *Plass et al.*, 1992; *Plass-Dülmer et al.*, 1993; *Donahue and Prinn*, 1993]. If of sufficient magnitude, the oceanic source of alkenes may have a substantial impact on the tropospheric chemistry over remote ocean regions. However, current estimates of global oceanic nonmethane hydrocarbons (NMHC) emissions are still very uncertain [cf. *Plass-Dülmer et al.*, 1995, and references therein]. This is mainly due to our lack of qualitative and quantitative understanding of the NMHC production mechanism. Although recent investigations gave principal insights into possible formation pathways [*Ratte et al.*, 1993, 1994, 1995; *Moore et al.*, 1994; *Milne et al.*, 1995; *McKay et al.*, 1996], the present knowledge is far from a precise quantitative description. It is not yet completely understood which parameters determine the oceanic alkene production.

We carried out several experiments in the laboratory and studied the formation of NMHC, including isoprene, in natural seawater. We investigated several parameters affecting the NMHC production, especially the wavelength dependence and the role of DOC. We will focus on C_2- to C_3-hydrocarbons, which represent more than 80% of total NMHC emissions from the oceans [*Plass-Dülmer et al.*, 1995].

2. Methods

2.1. Experimental Vessels, Seawater Used, and Bacterial Densities

The concentrations of NMHC dissolved in seawater were measured as a function of irradiation time for different spectral regions. For each experiment, several quartz glass vessels (HSQ 300) of about 2 L volume were filled with identically pretreated seawater and exposed to light of a certain wavelength range. Each vessel served as one sample and was analyzed (see below) after a certain exposure time. Details of vessels (cleaning procedure, material, and geometry) are given by *Ratte et al.* [1993]. Seawater samples from different regions in the North Atlantic, the North Sea, and the Arctic Sea were

[1]Now at Institut fur Stratosphärische Chemie, Jülich, Germany.
[2]Now at Centre for Atmospheric Chemistry and Department of Chemistry, York University, North York, Ontario, Canada.

Paper number 97JD03473.
0148-0227/98/97JD-03473$09.00

Table 1. Conditions of All Experiments Conducted in the Present Study

Spectral Range, nm	Irradiation Intensity W m^{-2}	Photon Flux, 10^{15} nm cm^{-2} s^{-1}	Origin of Seawater	DOC,* mg L^{-1}	Exposure Time, d	Name of Experiment
Dark	...	...	North Sea 1993	1.8	42	dark
300–420	30 ± 10	5.29	North Sea 1993	1.8	42	degassing
300–420	30 ± 10	5.29	North Sea 1993	1.8	10	O_2
300–420	30 ± 10	5.29	North Sea 1991	1.3	7	UV-1
300–420	30 ± 10	5.29	North Sea 1993	1.8	9	UV-2
300–420	30 ± 10	5.29	North Sea 1993 + FA†	1 (FA)‡	9	FA+1A
300–420	30 ± 10	5.29	North Sea 1993 + FA†	2 (FA)‡	9	FA+2A
300–420	30 ± 10	5.29	Arctic Sea	2.8	3	UV-3
300–420	30 ± 10	5.29	Arctic Sea + FA§	0.5 (FA)‡	5	FA+0.5B
300–420	30 ± 10	5.29	Arctic Sea + FA§	1 (FA)‡	5	FA+1B
300–420	30 ± 10	5.29	Arctic Sea + FA§	2 (FA)‡	5	FA+2B
320–800	35 ± 8	10.0	North Sea 1991	1.3	14	VIS-320–800
410–540	35 ± 8	8.03	Arctic Sea	2.8	10	VIS-410–540
410–540	35 ± 8	8.03	Arctic Sea + FA§	0.5 (FA)‡	9	FA+0.5C
410–540	35 ± 8	8.03	Arctic Sea + FA§	1 (FA)‡	9	FA+1C
410–540	35 ± 8	8.03	Arctic Sea + FA§	2 (FA)‡	9	FA+2C

*Total dissolved organic carbon, measured by high-temperature combustion oxidation (HTCO).
†Batch 1.
‡DOC consisting of fulvic acids (FA), nominal amount added.
§Batch 2.

used in several experiments (see Table 1). The water was stored without any pretreatment in 60 L polyethylene balloons at 4°C in the dark and filtered through 0.2 μm filters before the experiments started. If not mentioned otherwise, the water was not purged with any gas before the start of an experiment, in order to avoid a possible loss of volatile DOC. The filtration efficiency was checked by epifluorescence microscopy (100 mL subsamples from each quartz glass bottle, fixed with 10 mL 17% formalin and stored at 6°C). Generally, filtration reduced the number of bacteria in seawater down to about 1×10^4 cells/mL, compared to 10^6–10^7 cells/mL in unfiltered samples. Although the number of bacteria sometimes increased during the experiment (especially in dark samples; UV irradiation prevented bacterial growth), the bacterial density generally remained about 1 order of magnitude lower in filtered samples compared to unfiltered seawater.

2.2. NMHC Measurement

The water samples of nearly 2 L volume were transferred from the experimental vessels through a 0.6 μm glass fiber filter to a degassing device. About 750 mL were used to flush the connection lines, valves, etc.; then 1 L was filled into a stripping chamber and purged with helium for 30 min at a flow rate of about 100 mL/min. The stripping efficiencies were in the range of 94–99%. Subsequently, the NMHC were cryogenically concentrated from the purge gas at liquid nitrogen temperature and analyzed by flame ionization detector gas chromatography (FID/GC). All materials in contact with the sample were stainless steel or glass. The detection limits were below 7 pmol/L, and the reproducibilities of the measurements were about 10%. The analytical system is described in detail by *Rudolph et al.* [1989] and *Plass et al.* [1991].

2.3. DOC Measurements

The concentrations of DOC were measured by two different methods. The total amount of DOC was derived from high-temperature combustion oxidation (HTCO), as described by *Peltzer and Brewer* [1993], using a commercial analyzer (Ionics). The detection limit is 0.1 mg C/L; the analytical error is about 10%. DOC was also determined by wet chemical oxidation combined with UV irradiation using a 100 W mercury low pressure lamp (85% emission at 254 nm, 15% at 185 nm) (WCO/UV) using an instrument produced by Gräntzel Company, Karlsruhe, Germany, with a detection limit of about 0.03 mg C/L. For concentrations larger than 0.2 mg C/L the analytical error is about 10%; for lower concentrations it is about 40%. By this method only 20–30% of HTCO-DOC was detected.

2.4. Algal Culture

The development of NMHC concentrations in a nonaxenic batch culture of the diatom *Thalassiosira rotula* was measured as a function of time and compared to that in a cell free control. Two glass bottles of 25 L volume were filled with 20 L of 0.2 μm filtered seawater to which different nutrients were added; one served as control, the other was inoculated with 6×10^4 cells/L. Both vessels were closed with polyethylene foil to avoid contamination and incubated for 9 days at 14°C in a light:dark cycle of 12:12 (fluorescent lamps, Phillips TLM 65W/33RS, spectral range 320–750 nm). To minimize any possible loss of dissolved NMHC into the head space of the bottles, neither of the subsets was aerated. In order to prevent sedimentation of the algal cells the culture was shaken once a day; for reasons of comparability the control was treated in the same way. Subsequent to shaking, a sample of 2 L was taken from each vessel for NMHC analysis. The cell density in the culture was determined every day using an inverted microscope.

2.5. Irradiation Conditions

The quartz glass vessels were placed in a closed box (about 1 m × 0.5 m × 1 m) internally covered with aluminum foil. Fluorescent lamps (Phillips TD/D 18W/96 (320–800 nm), Phillips TL 20W 09/N (300–420 nm), and Phillips TL 20W/52 (410–540 nm)) provided irradiation of different, but partly overlapping, spectral ranges (Figure 1). In the following the three irradiation regimes are referred to as $UV_{300-420\,nm}$, $VIS_{320-800\,nm}$, and $VIS_{410-540\,nm}$.

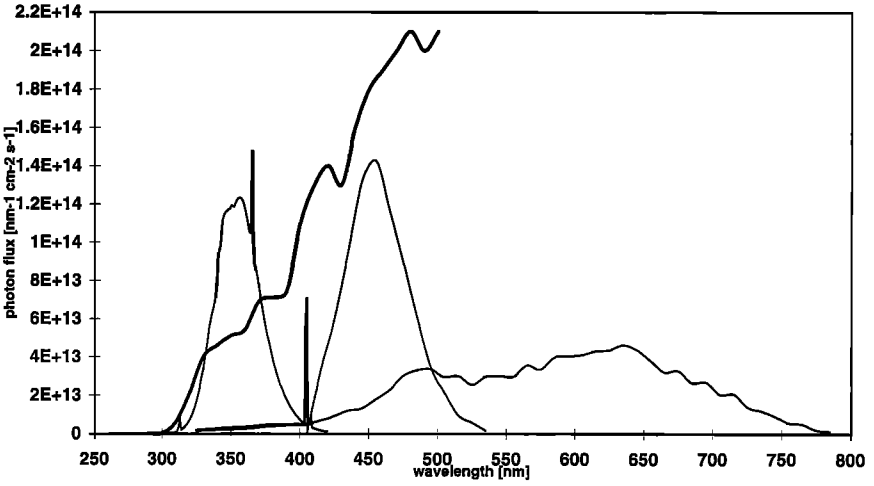

Figure 1. Actinic fluxes of fluorescent lamps used in experiments (thin solid lines; Phillips TD/D 18W/96 (320–800 nm), Phillips TL 20W 09/N (300–420 nm), Phillips TL 20W/52 (410–540 nm)) and mean global solar spectrum used for extrapolation (thick solid line).

The spectral distributions of the photon fluxes were measured with a spectroradiometer (resolution, 1 nm) described by *Müller* [1994] and *Müller et al.* [1995]. The instrument is equipped with a special sensor and recorded the actinic flux in the upper hemisphere of the box (2π sr).

Additionally, the spherically integrated irradiation intensity of either the upper or the lower hemisphere of the box was measured with a commercial solarimeter (Kipp and Zonen, range of measurement 250–2500 nm) and a filter radiometer developed by *Junkerman et al.* [1989], respectively. Thereby, the total sum of irradiation reaching the vessels was recorded, regardless of being directly irradiated or reflected. These measurements reveal a contribution of 83% from the upper hemisphere and 17% from the lower hemisphere to the total irradiation intensity inside the box. The spectral distribution of the irradiation was assumed to be identical in both hemispheres. The total irradiation intensities varied by ±30% depending on the horizontal and vertical position and the number of vessels placed in the box. Figure 1 gives the mean photon fluxes. The experiments took place under permanent illumination. The box was ventilated, but there was no thermal control. The temperature inside the box was about 26°C; the sample temperature was not measured. Dark samples were completely covered with aluminum foil and also placed in the box.

2.6. Rates of Increase

The experiments lasted between 7 and 42 days. Initial rates of increase were calculated by linear regression for the initial phase of each experiment (up to day 10). The significance of regression coefficients was statistically tested according to *Sachs* [1992]. For better comparability, the rates of increase were standardized to a DOC concentration of 1 mg L^{-1} (measured with HTCO). Due to the errors of regression coefficients and HTCO measurements, the total error of these standardized rates of increase is about 20%.

2.7. Calculation of Quantum Yields

Mean quantum yields for alkene production in the different wavelength ranges were calculated according to

$$\varphi = \frac{P_{\lambda 1}^{\lambda 2}}{\int_{\lambda 1}^{\lambda 2} A(\lambda)\alpha(\lambda)[\mathrm{DOC}]\, d\lambda} \quad (1)$$

where

P molecules produced, molec cm^{-3} s^{-1};
$A(\lambda)$ mean actinic flux, photons cm^{-2} s^{-1} nm^{-1};
$\alpha(\lambda)$ absorption coefficient, L cm^{-1} (mg DOC)$^{-1}$;
[DOC] DOC concentration (measured with HTCO), mg L^{-1};
λ wavelength, nm.

From the linear increase of alkene concentrations in the early phase of the experiments, it can be concluded that (initially) there is no loss of NMHC and thus the alkene production rate is identical to the rate of increase.

Generally, the absorption coefficient of DOC shows an exponential decrease with increasing wavelength. Depending on the origin of DOC, the individual absorption spectra of the seawater used in our experiments varied (Figure 2). They were measured in the wavelength range from 250 to 400 or 500 nm with a resolution of 5 nm or 10 nm, respectively (Kontron Phystech spectrometer, type Uvikon 860, and Perkin Elmer spectrometer, type 551). The number of photons absorbed was calculated for 1 nm intervals as product of the photon flux, the corresponding absorption coefficient, and the concentration of DOC. The following assumptions or simplifications were made: The mean path length of light through the water column is 20 cm; while passing these 20 cm, the irradiation intensity decreases due to wavelength dependent absorption by DOC; this was considered when calculating the total number of photons absorbed (the total loss of light intensity due to DOC absorption was at most 20%). We found evidence for a decrease of the DOC absorption coefficient and the concentration of a certain DOC fraction within the first 10 days of irradiation (see below). Since this was not further investigated and quantified, in a first approximation constant (initial) DOC absorption coefficients and DOC concentrations were used for calculation of quantum yields. The resulting quantum yields therefore will be lower limits.

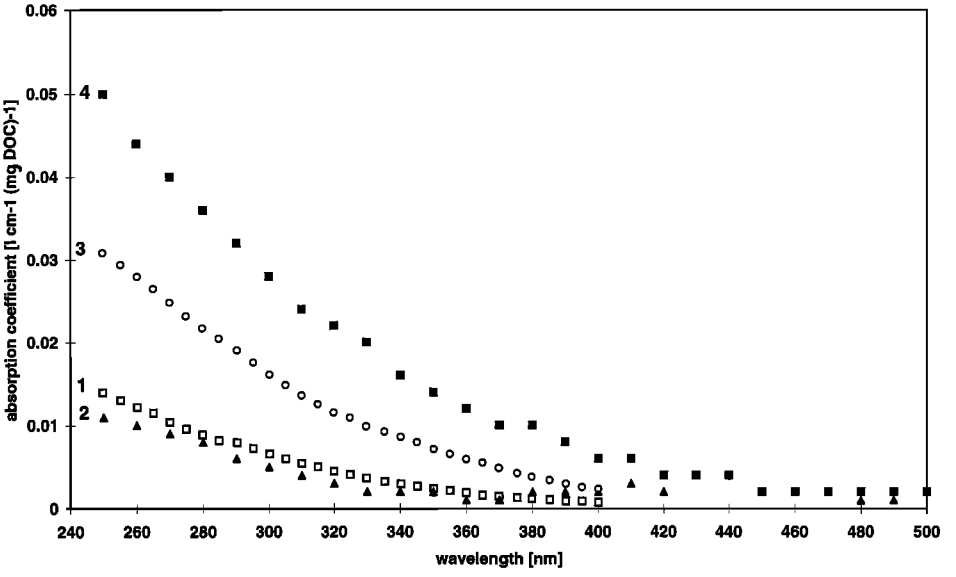

Figure 2. Absorption spectra of seawater used and of fulvic acids added (absorption coefficients per mg DOC L^{-1}). Sample 1 (open squares) is North Sea 1993; sample 2 (triangles) is Arctic Sea; sample 3 (circles) is fulvic acids, batch 1; sample 4 (solid squares) is fulvic acids, batch 2.

As a consequence of the uncertainties of the different variables involved in (1), error propagation leads to a total error of the resulting quantum yields of about 40–50% with the dominating error being the uncertainty of the photon flux.

2.8. Description of Experiments

Generally, the concentrations of NMHC dissolved in seawater were measured as a function of spectral range, exposure time, and origin and concentration of DOC (Table 1).

In some experiments an extract of fulvic acids (FA) from the Congo River was added to the seawater before irradiation started. Generally, 1 mg FA corresponded to 0.5 mg DOC (measured by HTCO). In the following, all results are related to the nominal amount of DOC added. Two different batches of FA extract were used which were characterized by different absorption spectra (Figure 2).

The light-independent NMHC production was measured in filtered seawater kept dark for 42 days. The effect of oxygen concentration on NMHC production rates was investigated in an independent experiment, named experiment O_2. About 25 L of seawater was purged with nitrogen (10 hours, 100 mL min^{-1}) until the O_2 concentration was below 0.1 mg L^{-1} (measured according to Winkler's method, [*Parsons et al.*, 1984]). Quartz glass vessels were filled with this nearly oxygen-free water or with seawater purged with synthetic air for the same time (oxygen concentration about 8 mg/L) and irradiated with $UV_{300-420\,nm}$ for 10 days.

A further experiment named "degassing" started with degassed seawater (purged with synthetic air, 17 hours, 1.5 L min^{-1}). Twenty-two quartz glass vessels with seawater were exposed to $UV_{300-420\,nm}$. During 27 days of exposure, eight samples were taken to measure NMHC concentration (subset degassing-initial). At day 27 the content of seven vessels was transferred into a stainless steel container and again purged with synthetic air (17 hours, 1.5 L min^{-1}) in order to remove volatile NMHC. Subsequently, these vessels were refilled, and the irradiation was continued for another 26 days (subset degassing-degassed). The remaining seven vessels of the set were irradiated for another 26 days without any treatment (subset degassing-continued).

3. Results

3.1. NMHC Concentrations in Algal Culture

In the culture of *Thalassiosira rotula*, increasing ethene concentrations were found, whereas the cell-free control showed approximately constant ethene concentrations (Figure 3a). The increase followed the exponential growth phase of the algae (days 3–5) with a time shift of 1 day. When the exponential growth phase of the algae had passed (after 6 days), the ethene concentration remained constant at about 120 pmol L^{-1}. The propene concentration (not shown) exhibited a very similar time dependence, with maximum values of about 40 pmol L^{-1}. We have no explanation for the increased cell density at day 9. The ethane (Figure 3b) and propane (not shown) concentrations showed irregular variations both in the control and in the culture, that is, no relation to cell density. For isoprene both in the culture and in the control, increasing concentrations up to a few tens of pmol L^{-1} were found (Figure 3c).

3.2. NMHC Concentrations and Rates of Increase in Filtered Seawater Samples

In filtered seawater kept dark for 41 days the concentrations of NMHC generally remained at a very low level compared to concentrations obtained in irradiated samples (experiment "dark", Table 2). The results obtained in unfiltered seawater kept dark up to 8 days [*Ratte et al.*, 1993] were very similar (Table 2). Nevertheless, in some cases the concentrations roughly doubled throughout the course of a dark experiment, implying a small dark production. The highest rate of increase measured in dark samples was 0.2 pmol ethene L^{-1} h^{-1} (mg DOC)$^{-1}$, corresponding to at most 10% of the measured rates of increase in irradiated samples. Therefore the rates of increase obtained in irradiated samples were not corrected for dark production rates.

The NMHC concentrations in irradiated seawater samples depended on substance, spectral range, and origin and concentration of DOC. For ethene and propene after 10 days of irradiation with $UV_{300-420\,nm}$, concentrations of several thousands of pmol L^{-1} were reached (Figure 4a (only ethene is shown), squares and diamonds). The individual rates of increase for one substance differed to some extent, depending on the origin of seawater and DOC (Table 3). For North Sea water, rates of increase of about 12 (ethene) and 5 (propene) pmol L^{-1} h^{-1} (mg DOC)$^{-1}$ were obtained; the rates of increase measured in Arctic Sea water were about 40% enhanced (ethene: 16 pmol L^{-1} h^{-1} (mg DOC)$^{-1}$; propene: 7.5 pmol L^{-1} h^{-1} (mg DOC)$^{-1}$). Under irradiation with $VIS_{320-800\,nm}$ the maximum concentrations after 10 days were only a few hundred pmol L^{-1} (Figure 4a, ethene: triangles; propene: not shown). The corresponding rates of increase were only about 15% of those for $UV_{300-420\,nm}$ (Table 3, ethene: 1.8 pmol L^{-1} h^{-1} (mg DOC)$^{-1}$; propene; 0.8 pmol L^{-1} h^{-1} (mg DOC)$^{-1}$). In the case of $VIS_{410-540\,nm}$ the ethene and propene concentrations remain nearly constant (Figure 4a, circles) and no statistically significant rates of increase were found (Table 3). In each experiment the ethene formation rate was roughly twice that of propene.

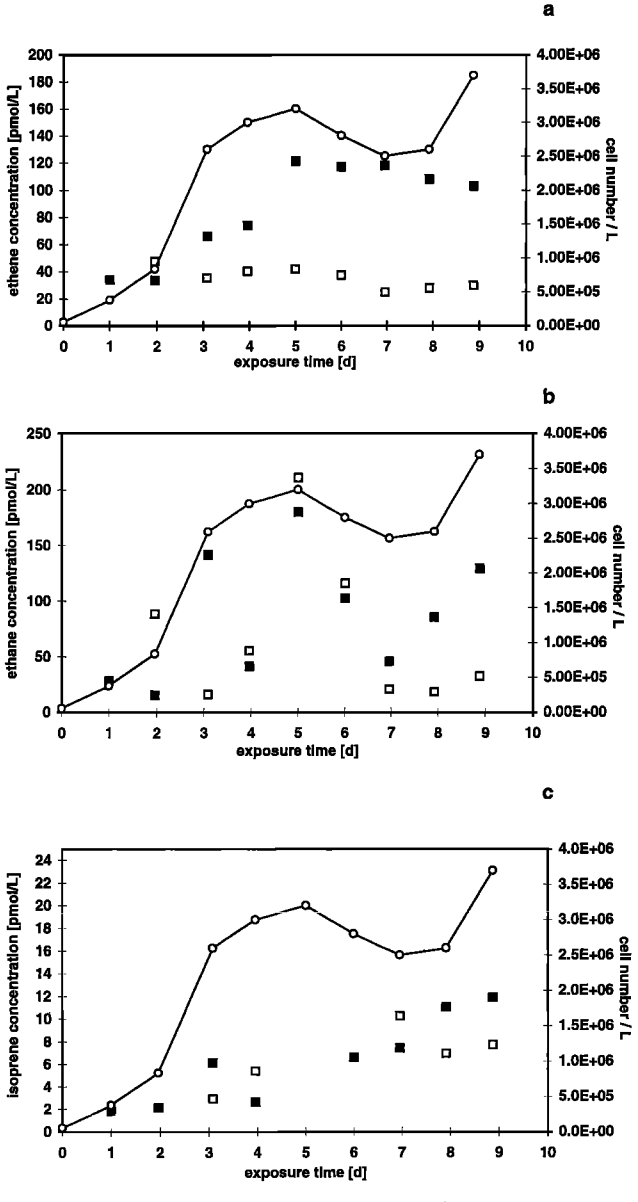

Figure 3. (a) Ethene, (b) ethane, and (c) isoprene concentration in a culture of the diatom *Thalassiosira rotula* (solid squares) and in a cell-free control (open squares) as function of time; circles denote cell number.

Table 2. Nonmethane Hydrocarbon Concentrations in Seawater Samples Kept Completely Dark

Exposure Time, h	Ethene	Propene	Ethane	Propane	Isoprene
	Experiment Dark, Filtered Seawater				
0	33	14	12	4	2
73	170*	67*	15	8	6
143	51	18	13	4	7
239	61	24	18	4	8
359	60	23	143*	136*	8
552	64	19	29	24	4
986	68	21	25	24	6
	Ratte et al. [1993] Experiment 1, Unfiltered Seawater				
0	55	27	19	8	n.d.
21	62	32	28	10	n.d.
94	70	30	31	11	n.d.
138	83	30	33	11	n.d.
180	98	48	36	16	n.d.
	Ratte et al. [1993] Experiment 2, Unfiltered Seawater				
0	48	25	13	8	n.d.
53	59	34	39	15	n.d.
96	63	30	27	11	n.d.
144	62	29	27	12	n.d.

Values are in pmol L^{-1}. For the *Ratte et al.* [1993] experiments, North Atlantic seawater was used (DOC = 1.7 mg L^{-1}). Here n.d. denotes not determined.

*Not considered for regression analysis (statistical test for outliers [*Sachs*, 1992]).

For ethane and propane the concentrations were in the range of a few tens to 150 pmol L^{-1} regardless of irradiation regime (Figure 4b), with an occurrence of several outliers (due to scaling, they are not all shown in Figure 4b). Since we have no explanation for this phenomenon except contamination, the outlier values were eliminated before regression analysis. In most cases the obtained rates of increase were statistically not significant.

Isoprene concentrations were only measured in two experiments using $UV_{300-420\,nm}$. Generally, the isoprene concentrations were much lower than those of other hydrocarbons (about 5–25 pmol L^{-1}, Figure 4c). The highest rate of increase obtained was 0.02 pmol L^{-1} h^{-1} (mg DOC)$^{-1}$ (Figure 4c, open diamonds).

The addition of fulvic acids to natural seawater and subsequent irradiation with $UV_{300-420\,nm}$ led to enhanced formation rates of ethene (Figure 5a) and propene (not shown) compared to seawater containing only natural oceanic DOC. The rates of increase per milligram DOC as fulvic acids were very similar to those per milligram oceanic DOC. They increased linearly with amount of fulvic acids added (Table 3). Irradiation with $VIS_{410-540\,nm}$ caused a statistically significant increase of ethene and propene concentrations in seawater with fulvic acids added, as opposed to seawater containing only oceanic DOC and irradiated with $VIS_{410-540\,nm}$ (Table 3). The rates of increase from fulvic acids under $VIS_{410-540\,nm}$ were about 6–7 times lower than those for $UV_{300-420\,nm}$. In the case

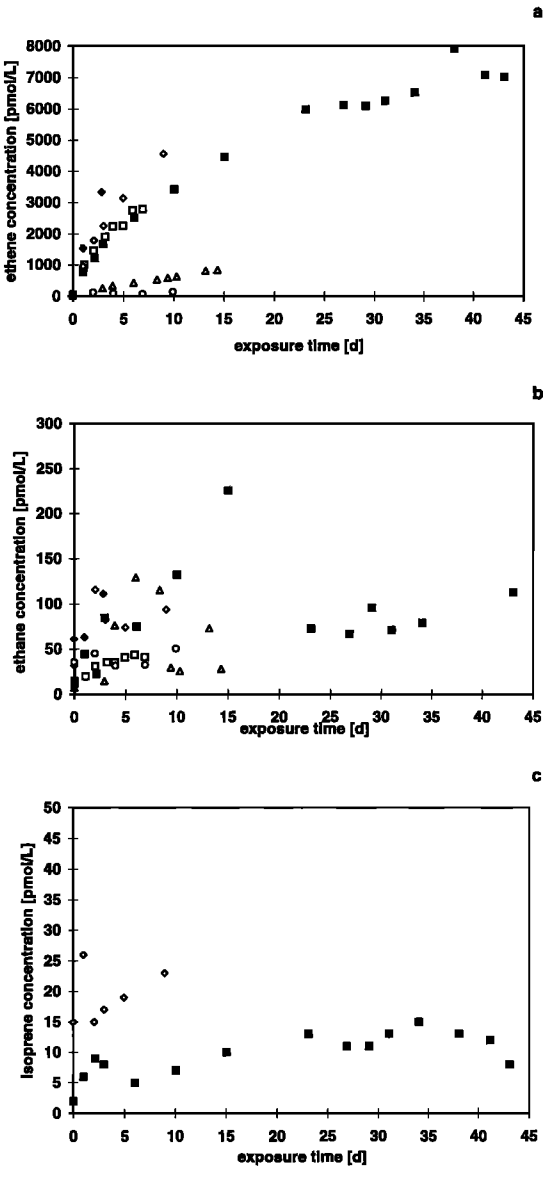

Figure 4. Concentration of (a) ethene, (b) ethane, and (c) isoprene in filtered, irradiated seawater samples as a function of irradiation time. Squares and diamonds denote exposure to UV light (solid squares: experiment degassing; open squares: experiment UV-1; open diamonds: experiment UV-2; filled diamonds: experiment UV-3); triangles denote exposure to $VIS_{320-800\,nm}$; and circles denote exposure to $VIS_{410-540\,nm}$. The concentration of isoprene was only measured in the experiments UV-2 and degassing. For names and conditions of experiments, see Table 1.

of $VIS_{410-540\,nm}$ a linear relationship between rate of increase and amount of fulvic acids added was obvious only for propene and less evident for ethene (Table 3).

In contrast to seawater containing only oceanic DOC, the concentrations of ethane and propane exhibited a continuous increase in the subsets with fulvic acids added and irradiated with $UV_{300-420\,nm}$ (Figure 5b, only ethane shown). However, no dependence on fulvic acid concentration was observed. The concentrations of isoprene were not affected by addition of fulvic acids and remained constant throughout the exposure time (Figure 5c).

3.3. Degassing Experiment

Ethene and propene were nearly completely removed by the degassing procedure (ethene: from 6126 pmol L^{-1} down to 12 pmol L^{-1}; propene: from 3700 pmol L^{-1} down to 8 pmol L^{-1}). Subsequent irradiation of the degassed samples evoked an increase of alkene concentrations. For ethene the rate of increase after degassing was about 30% lower than the initial rate of increase but exceeded that of continued irradiation by about 30% (Table 3). For propene the rates of increase in the different experimental subsets were very similar (Table 3). Neither the alkanes nor isoprene showed any systematic concentration increase.

3.4. Quantum Yields

The quantum yields were in the range of 10^{-7} to 10^{-9}. The quantum yields obtained for a certain spectral range varied slightly depending on the origin of seawater and of DOC (Table 3). In most cases, the quantum yield for ethene production was twice that for propene production. For DOC of the same origin, the quantum yields for $VIS_{320-800\,nm}$ were very similar to those measured for $UV_{300-420\,nm}$. In contrast, the quantum yields for $UV_{300-420\,nm}$ generally exceeded those obtained in $VIS_{410-540\,nm}$, with the extent of the difference depending on the origin of DOC. For example, the relation of quantum yields in $UV_{300-420\,nm}/VIS_{410-540\,nm}$ varied between a factor of about 2 (FA in Arctic Sea water) and a factor of about 100 (Arctic Sea water) for ethene (Table 3).

3.5. DOC Concentrations and Absorption Coefficients

The HTCO DOC measurements exhibited no statistically significant change during exposure time, either in samples irradiated with $UV_{300-420\,nm}$ (Figure 6a, open symbols) or in those kept dark (not shown). Nevertheless, there occurred elevated HTCO DOC concentrations after day 40. Unfortunately, the experiments were terminated just at this time, and the statistical evaluation of the existing data set does not indicate that the change is statistically significant. In contrast, the DOC concentrations measured by WCO/UV exhibited a statistically highly significant decrease of 75% within 41 days if the samples were irradiated with $UV_{300-420\,nm}$ (Figure 6a, solid symbols). In dark samples the WCO/UV DOC concentrations showed a slight decrease (initial concentration: 0.29 mg L^{-1}; final concentration after 41 days: 0.23 mg L^{-1}, not shown); however, due to the small database ($n = 3$) this could not be judged statistically.

The absorption measurements clearly reveal a decrease of absorption coefficient throughout the course of an experiment under $UV_{300-420\,nm}$, indicating a change in DOC concentration and/or composition due to irradiation (Figures 6b, 7a, and 7b). If the samples were kept dark, the absorption spectra changed by less than 10% within 41 days (not shown).

4. Discussion

According to the existing literature, NMHC in seawater may be formed by two different mechanisms: They may be of biological origin, for example, directly released by phytoplankton, or they may be produced photochemically from dissolved organic carbon, with the DOC being probably of biological origin [*Wilson et al.*, 1970; *Hannan et al.*, 1977; *Schobert and Elstner*, 1980; *Lee and Baker*, 1992; *McKay et al.*, 1996; *Ratte et al.*, 1993, 1994; *Riemer et al.*, 1996]. The results obtained in the present

Table 3. Alkene Production Rates and Quantum Yields Obtained in the Present Paper

Spectral Region, nm	Experiment	Origin of Water/DOC	Rate of Increase, pmol L^{-1} h^{-1} (mg DOC)$^{-1}$		Quantum Yield, 10^{-8}	
			Ethene	Propene	Ethene	Propene
300–420	UV-1	North Sea 1991	12.1	5.3	8.5	3.7
	UV-2	North Sea 1993	11.2	5.3	8.1	3.8
	UV-3	Arctic Sea	16	7.5	17	7.9
	FA+1A	FA (batch 1) in North Sea 1993‡	12.7*	5.9*	3.5†	1.6†
	FA+2A	FA (batch 1) in North Sea 1993‡	12.2*	5.4*	4.0†	1.8†
	FA+0.5B	FA (batch 2) in Arctic Sea§	14.0*	8.6*	1.8†	1.1†
	FA+1B	FA (batch 2) in Arctic Sea§	13.8*	6.9*	1.0†	1.0†
	FA+2B	FA (batch 2) in Arctic Sea§	13.0*	10.1*	2.4†	1.9†
	O_2 < 0.1 mg L^{-1}	North Sea 1993	13.4	7.2	9.5	5.1
	O_2 = 8 mg L^{-1}	North Sea 1993	11.9	7.4	8.5	5.3
	Degassing					
	-initial	North Sea 1993	7.3	4.1	5.2	2.9
	-degassed	North Sea 1993	5.1	4.3	16	14
	-continued	North Sea 1993	3.7	3.7	7.6	7.6
320–800	VIS-320–800	North Sea 1991	1.8	0.8	13.0	5.8
410–540	VIS-410–540	Arctic Sea	0.021 n.s.	0.032 n.s.	0.11	0.16
	FA+0.5C	FA (batch 2) in Arctic Sea	3.2*	0.8*	1.0†	0.3†
	FA+1C	FA (batch 2) in Arctic Sea	2.2*	0.8*	0.7†	0.3†
	FA+2C	FA (batch 2) in Arctic Sea	1.8*	0.8*	0.6†	0.3†

FA denotes fulvic acids; n.s. denotes statistically not significant.
*Only production from fulvic acids added, that is, difference from control without FA added.
†Quantum yield of production from fulvic acids added.
‡Control: UV-2.
§Control: UV-3.

study also point to different production mechanisms for alkanes, for ethene and propene, and for isoprene.

For alkanes, no consistent picture could be obtained. The alkane concentrations generally exhibited irregular fluctuations and several outliers, the reason for which could not be identified. From our experiments we therefore cannot conclude how alkanes are produced in seawater, except the general statement that the factors determining their concentrations are different from those for ethene, propene, and isoprene.

Our experiments with cell-free seawater clearly indicate a photochemical production of ethene and propene from dissolved organic carbon. Also, in a culture of diatoms the concentrations of ethene and propene increased compared to a cell-free control. However, in spite of an exponential growth rate of the algae, the rates of increase of alkene concentrations were low (ethene: 0.9 pmol L^{-1} h^{-1}; propene: 0.2 pmol L^{-1} h^{-1}) compared to those obtained in filtered seawater samples (see Table 3). Moreover, in view of the spectral range used in this experiment a major part of these alkenes probably are of photochemical origin. Since in the cell-free control no increase of alkene concentrations was observed, a photochemical alkene production in the algal culture must be based on DOC released by the algae. This experiment therefore demonstrates the indirect role of phytoplankton in the alkene production process rather than a direct biological alkene production.

For isoprene we found increasing concentrations in a culture of the marine diatom *Thalassiosira rotula*, but also in the cell-free control. The origin of the isoprene produced in this experiment therefore cannot be clearly identified. However, the extent of photochemical isoprene production in filtered irradiated samples was found to be 2 orders of magnitude lower than that of ethene and propene. Recent findings of other authors provide evidence that isoprene is not produced photochemically, but biologically during the phytoplankton life cycle [*Bonsang et al.*, 1992; *Moore et al.*, 1994; *Milne et al.*, 1995; *McKay et al.*, 1996].

In the following, we will focus on the photochemical formation pathway leading to the production of ethene and propene. The results might be influenced by oxygen consumption, DOC consumption, or a possible photochemical alkene destruction.

The rates of increase for ethene and propene were very similar regardless of oxygen concentration (experiment O_2, Table 3). Experimental artifacts due to changing oxygen concentrations throughout the course of an experiment therefore seem to be negligible, at least for the range of oxygen concentrations investigated (0.1–8 mg L^{-1}). Generally, both aeration with synthetic air or purging with N_2 before irradiation not only affect oxygen concentration, but also may cause a loss of volatile compounds, that is, possible alkene precursors, and thus may affect the rates of increase for alkenes. When comparing rates of increase in degassed and not degassed samples (degassing-initial, O_2, UV-2, Table 3), no clear tendency can be seen, and in most cases the differences fell within the range of error of the individual rates of increase. Moreover, the absorption spectra measured just before and after degassing were very similar (not shown).

The tapering off of alkene concentrations which occurred under long time exposure with $UV_{300-420\,nm}$ (Figure 4a) may be due to a depletion of alkene precursors with increasing irradiation time or a photochemical alkene destruction. We found hints supporting both explanations. Generally, the DOC measurements reveal a decrease of a certain fraction of DOC which can be detected by WCO/UV and absorption measurement (Figures 6a and 6b). Different DOC concentrations would explain the slight difference between the rates of increase of ethene in the subsets degassing-initial and degassing-degassed (Table 3), which started with identical (very low) alkene concentrations. Since the propene production rate remains unaffected in these subsets, this may indicate the exis-

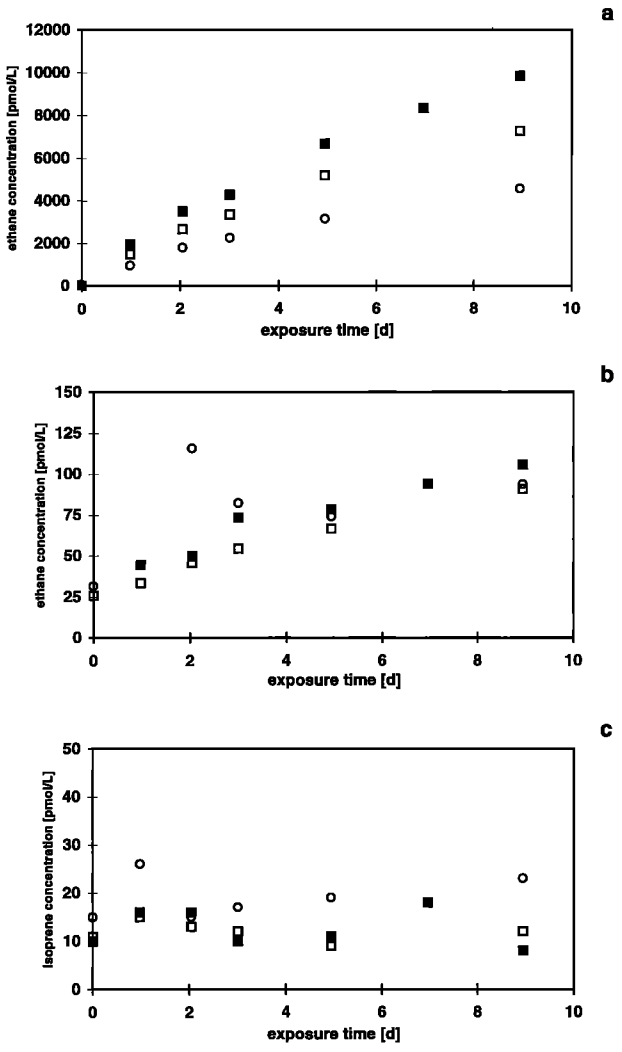

Figure 5. Concentration of (a) ethene, (b) ethane, and (c) isoprene in seawater with fulvic acids added and in control without addition of DOC (open circles: experiment UV-2), as a function of exposure to UV light (open squares: experiment FA+1A, addition of 2 mg L^{-1} of fulvic acids, corresponding to 1 mg L^{-1} DOC; solid squares: experiment FA+2A, addition of 4 mg L^{-1} of fulvic acids, corresponding to 2 mg L^{-1} DOC).

tence of different DOC pools for ethene and propene production or a slower rate of DOC conversion into propene than into ethene. On the other hand, when comparing the rates of increase in subsets with identical DOC pools but very different alkene concentrations (subset degassing-degassed compared to degassing-continued, Table 3), for ethene the rate of concentration increase in seawater obviously depends on the overall concentration level: The higher the starting concentration, the lower the further increase. This may be explained by a photochemical alkene destruction. Such a process would be proportional to the alkene concentration and therefore would be more important, the higher the alkene concentrations were.

However, regardless of possible precursor consumption or alkene destruction in our experiments, the tapering off of alkene concentrations was first detectable after 8 to 10 days of irradiation. Therefore the initial increase measured in our experiments will not be influenced by this problem.

The alkene production rate was found to be a function of spectral range and of the origin of seawater and of DOC. The effect of DOC depends on the spectral range: In $UV_{300-420\,nm}$ the production rates for ethene and propene in seawater containing DOC from the North Sea, from the Arctic Sea, or as fulvic acids were very similar (Table 3). In contrast, in $VIS_{410-540\,nm}$ the production rates based on DOC from the Arctic Sea water and on fulvic acids differed by a factor of 100 (Table 3). However, the differences between the corresponding production efficiencies, measured as quantum yields, were less extreme. Depending on the origin of DOC they varied between a factor of 2 and a factor of 10. Generally, the rates of increase and the quantum yields for ethene were about 2 times those of propene (Table 3).

The quantum yields obtained in the present study are not wavelength resolved, but are mean values for a broad wavelength range. Actually, they are only valid for the corresponding emission spectrum for which they were calculated. Since the emission spectra of the fluorescent lamps differ considerably from the real solar actinic flux (Figure 1), the mean quantum yields obtained in our experiments can only provide a rough estimate for the quantum yields under natural solar irradiation. As far as we know, up to now no quantum yields for photochemical alkene production are available in the literature. The only data we are aware of are wavelength-specific quantum yields obtained by D. D. Riemer et al. (unpublished data, 1997), who measured photochemical alkene production

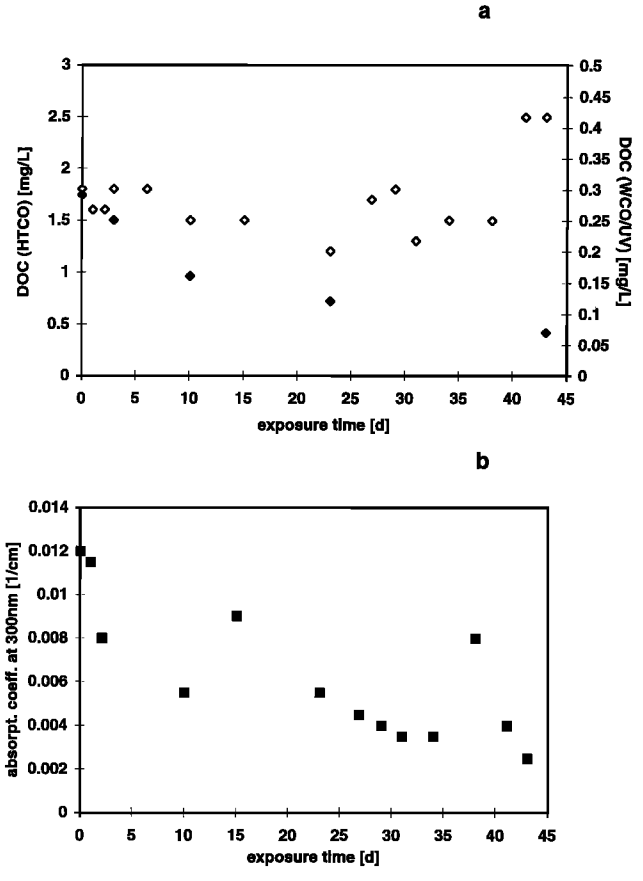

Figure 6. DOC concentrations (open symbols: high-temperature combustion oxidation; solid symbols: wet chemical oxidation/UV) and (b) absorption coefficient at $\lambda = 300$ nm in seawater samples as a function of exposure time to $UV_{300-420\,nm}$ (experiment degassing).

rates from DOC of different origin for individual wavelengths between 280 nm and 366 nm. They found quantum yields for ethene and propene production in the range of 10^{-8} to 10^{-7} depending on the origin of DOC, that is, in the same range as the quantum yields obtained in the present study. The highest quantum yields were obtained for Gulf stream water; the lowest were found in water of the Banana River. Generally, the quantum yields exhibited an exponential decrease with increasing wavelength and became nearly zero at wavelengths of about 420 nm (Figure 8; the only exception to exponential decrease occurred for propene in Gulf stream water). Such an exponential wavelength dependence of quantum yield would explain our experimental finding of statistically significant production rates under $VIS_{320-800\,nm}$ in contrast to those under $VIS_{410-540\,nm}$: The alkene production rates found in $VIS_{320-800\,nm}$ then most probably are due to the wavelength range up to 420 nm. We will use the data of Riemer et al. to calculate alkene production rates in the ocean (see below).

Since emission into the atmosphere is the dominant loss process for alkenes in seawater [*Plass et al.*, 1992; *Ratte et al.*, 1993], estimates of the oceanic source strength for alkenes can be based on production rates. The oceanic alkene production rates can be calculated according to

$$d[\text{alkene}](\lambda)/dt\, d\lambda = A(\lambda, l)\alpha(\lambda)[\text{DOC}]\varphi(\lambda) \quad (2)$$

where

$A(\lambda, l)$ actinic flux at wavelength λ and depth l, nm^{-1} cm^{-2} s^{-1};
$\alpha(\lambda)$ absorption coefficient, L cm^{-1} (mg DOC)$^{-1}$;
[DOC] DOC concentration, mg L^{-1};
$\varphi(\lambda)$ quantum yield.

Assuming

$$A(\lambda, l) = A_{sol}(\lambda)\, \exp\,(-E(\lambda)l) \quad (3)$$

where A_{sol} is actinic flux at ocean surface and $E(\lambda)$ is extinction at wavelength λ, we obtain

$$d[\text{alkene}](\lambda)/dt\, d\lambda = A_{sol}(\lambda)\, \exp\,(-E(\lambda)l)\alpha(\lambda) \cdot [\text{DOC}]\varphi(\lambda) \quad (4)$$

Integration of (4) leads to a column-integrated production rate P_{col} per unit of ocean area:

$$P_{col} = \int d[\text{alkene}](\lambda)/dt\, d\lambda dl = A_{sol}(\lambda)\alpha(\lambda) \cdot [\text{DOC}]/E(\lambda)\varphi(\lambda) \quad (5)$$

If in a first approximation light extinction is assumed to be caused only by DOC absorption, that is, $E = \alpha(\lambda)[\text{DOC}]$, (5) can be simplified to

$$P_{col}(\lambda) = A_{sol}(\lambda)\varphi(\lambda) \quad (6)$$

Hence all photons penetrating the sea surface are assumed to contribute to alkene production, and production rates can be calculated based on a total ocean surface of 361×10^6 km^2.

A mean actinic flux (24 hours) reaching the ocean surface (Figure 8) was calculated as follows: Starting with the extraterrestric flux [*World Meteorological Organization (WMO)* 1985], the number of photons passing through an atmosphere of global mean conditions (U.S. Standard Atmosphere, 1976) was calculated for different solar zenith angles using the photon flux model by *Röth* [1992]. Then, the diurnal cycle (12 hours) of the actinic flux at sea level at latitude 33° was averaged for each wavelength interval separately in order to obtain a global mean actinic flux spectrum. By this procedure the wavelength-dependent weighting factor of the averaging procedure was considered. The actinic flux was determined every 10 nm including absorption of O_3 and NO_2 (with the absorption spectra given by *WMO* [1985]) as well as Rayleigh and Mie scattering for clear sky conditions. In a first approximation the albedo of sea surface was neglected, and all photons reaching the sea surface were assumed to penetrate into the water column.

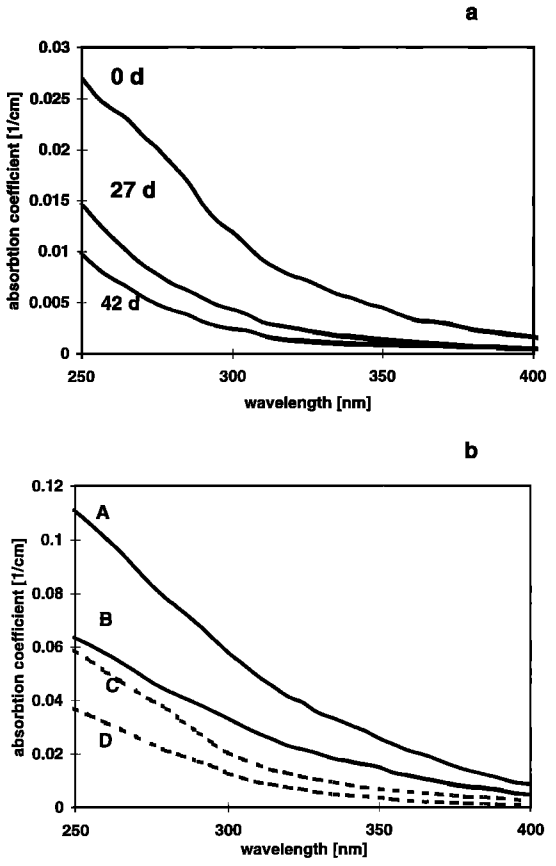

Figure 7. (a) Absorption spectra (from top to bottom) of seawater samples before irradiation and after 27 days and after 42 days of irradiation with $UV_{300-420\,nm}$ (experiment degassing). (b) Absorption spectra of seawater with fulvic acids (FA) added before irradiation (solid lines, A: FA+2A (i.e., 2 mg L^{-1} DOC as FA added), B: FA+1A (i.e., 1 mg L^{-1} DOC as FA added), and after 9 days of irradiation with $UV_{300-420\,nm}$ (dashed lines, C: FA+2A, D: FA+1A).

To sum up, for calculating global alkene production rates we assume (1) all photons reaching the sea surface penetrate into the water and (2) DOC is the only absorbing component. The resulting number of photons that are relevant for alkene production therefore is an upper limit.

The wavelength interval of 290–420 nm was assumed as the relevant spectral range for alkene production. In a first approach, mean quantum yields of 8.1×10^{-8} (ethene) and 3.8×10^{-8} (propene) were used, as obtained in experiment UV-2 (Figure 8). As already pointed out in section 2.7, these quantum yields are lower limits, which will partly compensate for the overestimation of the number of photons absorbed.

To investigate how the irradiation conditions based on our

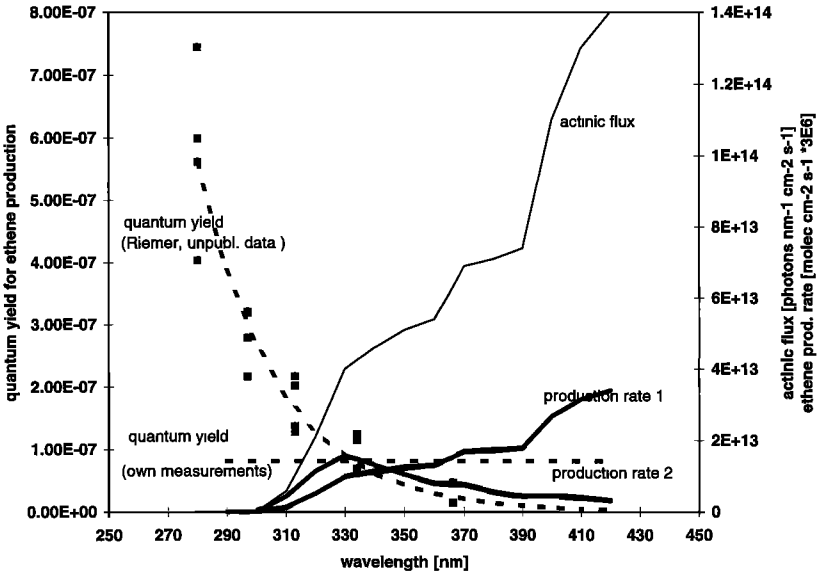

Figure 8. Mean global solar flux at sea surface (thin solid line, calculated according to *Röth* [1992], see text), quantum yields for ethene production (squares denote measurements of D. D. Riemer et al. (unpublished data, 1997) in four different water types (a fit to these data is given by the dashed line); lower straight dashed line: mean quantum yield obtained in the present study in experiment UV-2), and the resulting global oceanic ethene production rates (thick solid lines; production rate 1 is based on mean quantum yield; production rate 2 is based on data of Riemer et al.).

assumption compare to real oceanic conditions, we calculated the penetration depths of light for the spectral region of 300–420 nm. Assuming DOC to be the only absorbing component, a mean global solar flux (see above), a mean oceanic DOC concentration of 1.5 ± 0.5 mg L^{-1} [*Druffel et al.*, 1992; *De Baar et al.*, 1993; *Thomas et al.*, 1995], and a DOC absorption spectrum as measured for North Sea water (experiment UV-2), the corresponding penetration depths ($1/e$) vary between 1 m and 12 m. They are in the same range as those given in the literature; for example, the mean penetration depth for 350 nm can vary between 0.25 m (coastal water, type 9) and 15 m (Sargasso Sea, open ocean water, type I) [*Gordon and McCluney*, 1975] (water types as classified by *Jerlov* [1976]). Thereby for the values from the literature the corresponding attenuation coefficients are sum parameters which do not distinguish between absorption by DOC and by other absorbers.

The extrapolation of global alkene production rates based on the quantum yields obtained in the present study results in 0.93 μg m^{-2} h^{-1} (corresponding to 2.95 Mt yr^{-1}) for ethene and 0.66 μg m^{-2} h^{-1} (corresponding to 2.07 Mt yr^{-1}) for propene. For comparison we used the quantum yields measured by D. D. Riemer et al. for four different water types (unpublished data, 1997), for which a mean fit was calculated as shown in Figure 8 (for ethene the correlation coefficient R^2 was 0.92; for propene it was only 0.64 due to an outlying data point). This results in production rates of 0.26 μg m^{-2} h^{-1} for ethene (corresponding to 0.84 Mt yr^{-1}) and 0.31 μg m^{-2} h^{-1} for propene (corresponding to 0.99 Mt yr^{-1}).

Figure 8 shows the contribution of the different wavelengths to ethene production. Under the assumption of wavelength-resolved quantum yields (production rate 2 in Figure 8), the wavelength range around 330 nm can be identified to be most efficient for alkene production.

Plass-Dülmer et al. [1995] estimated global oceanic C_2 to C_4 emission rates of 2.1 Mt per year with an upper limit of 5.5 Mt per year. Thereby the contribution of ethene is about 40%, corresponding to 0.9 Mt yr^{-1} with an upper limit of 2.2 Mt yr^{-1}. The global oceanic C_2 and C_3 alkene production rates estimated in the present study closely correspond to these data and thus confirm the conclusion of *Plass-Dülmer et al.* [1995] that the global oceanic source strength for alkenes is much lower than previously estimated. In fact, it seems negligible compared to global volatile organic carbon emissions of about 1150 Mt C yr^{-1} [*Guenther et al.*, 1995]. Nevertheless, depending on local conditions such as solar flux and biological activity, individual local production rates can differ from global oceanic source strength. In the present investigation the most important factors affecting alkene production rates and thus locally restricted atmospheric chemistry are identified and quantified.

5. Conclusions

The present investigation provides a quantitative relation between the photochemical production rate of alkenes, DOC concentration, and actinic flux. The production is determined by the concentration and reactivity of DOC, the incoming light intensity in the near UV and short visible light, and the wavelength-specific quantum yields. Only if DOC is the primary absorber would the total column-integrated alkene production rate be independent of the light penetration depth. Otherwise, the relation between the different light absorbers will play a key role in the alkene production rate. Depending on water type and biological activity the contribution of DOC to actual light extinction may be highly variable. We therefore would expect potentially high alkene production in ocean water with high concentrations of reactive DOC, but otherwise low light extinction. Important DOC sources are riverine input and biological activity, which both are also sources for light-absorbing phytoplankton and particles. Therefore the alkene

production rate is not strictly proportional to the DOC concentration nor to the biological activity.

Acknowledgments. We greatly appreciate the assistance of A. Kraus and M. Müller with characterization of irradiation conditions and of E. P. Röth with modeling a global actinic flux. Many thanks to D. Riemer for providing unpublished data and for interesting discussions. We are grateful to A. Dickmeis and F. Haegel for assistance with WCO/UV DOC analytics and absorption measurements and to B. Oligschleger for assistance with one of the experiments.

References

Bonsang, B., M. Kanakidou, G. Lambert, and P. Monfray, The marine source of C_2-C_6 aliphatic hydrocarbons, *J. Atmos. Chem.*, *6*, 3–20, 1988.

Bonsang, B., C. Polle, and G. Lambert, Evidence for marine production of isoprene, *Geophys. Res. Lett.*, *19*, 1129–1132, 1992.

De Baar, H. J. W., C. Brussaard, J. Hegeman, J. Schijf, and M. H. C. Stoll, Sea trials of three different methods for measuring nonvolatile dissolved organic carbon in seawater during the JGOFS North Atlantic pilot study, *Mar. Chem.*, *41*, 145–152, 1993.

Donahue, N. M., and R. G. Prinn, In situ nonmethane hydrocarbon measurements on SAGA 3, *J. Geophys. Res.*, *98*, 16,915–16,932, 1993.

Druffel, E. R. M., P. M. Williams, J. E. Bauer, and J. R. Ertel, Cycling of dissolved and particulate organic matter in the open ocean, *J. Geophys. Res.*, *97*, 15,639–15,659, 1992.

Ferek, R., and M. O. Andreae, Photochemical production of carbonyl sulfide in marine surface waters, *Nature*, *307*, 148–150, 1984.

Gordon, H. R., and W. R. McCluney, Estimation of the depth of sunlight penetration in the sea for remote sensing, *Appl. Opt.*, *14*, 413–416, 1975.

Guenther, A., et al., A global model of natural volatile organic compound emissions, *J. Geophys. Res.*, *100*, 8873–8892, 1995.

Hannan, P. J., R. A. Lamontagne, J. W. Swinnerton, and C. Patouillet, Algae, ultraviolet light, and the production of trace gases, *Rep. 3664*, Nav. Res. Lab., Washington, D. C., 1977.

Jerlov, N. G., *Marine Optics*, *Elsevier Oceanogr. Ser.*, vol. 14, Elsevier, New York, 1976.

Junkermann, W., U. Platt, and A. Volz-Thomas, A photoelectric detector for the measurement of photolysis frequencies of ozone and other atmospheric molecules, *J. Atmos. Chem.*, *8*, 202–227, 1989.

Kieber, D. J., J. McDaniel, and K. Mopper, Photochemical source of biological substrates in sea water: Implications for carbon cycling, *Nature*, *341*, 637–639, 1989.

Kieber, R. J., X. Zhou, and K. Mopper, Formation of carbonyl compounds from UV-induced photodegradation of humic substances in natural waters: Fate of riverine carbon in the sea, *Limnol. Oceanogr.*, *35*, 1503–1515, 1990.

Lee, R. F., and J. Baker, Ethylene and ethane production in an estuarine river: Formation from the decomposition of polyunsaturated fatty acids, *Mar. Chem.*, *38*, 25–36, 1992.

McKay, W. A., M. F. Turner, B. M. R. Jones, and C. M. Halliwell, Emissions of hydrocarbons from marine phytoplankton—Some results from controlled laboratory experiments, *Atmos. Environ.*, *30*, 2583–2593, 1996.

Milne, P. J., D. D. Riemer, R. G. Zika, and L. E. Brand, Measurement of vertical distribution of isoprene in surface sea water, its chemical fate and its emission from several phytoplankton monocultures, *Mar. Chem.*, *48*, 237–244, 1995.

Moore, R. M., and O. C. Zafiriou, Photochemical production of methyl iodide in seawater, *J. Geophys. Res.*, *99*, 16,415–16,420, 1994.

Moore, R. M., D. E. Oram, and S. A. Penkett, Production of isoprene by marine phytoplankton cultures, *Geophys. Res. Lett.*, *21*, 2507–2510, 1994.

Mopper, K., Zhou, X., R. J. Kieber, D. J. Kieber, R. J. Sikorski, and R. D. Jones, Photochemical degradation of dissolved organic carbon and its impact on the oceanic carbon cycle, *Nature*, *353*, 60–62, 1991.

Müller, M., Messungen der aktinischen ultravioletten Strahlung und der Ozonphotolysefrequenz in der AtmosphSre mittels Filterradiometrie und Spektralradiometrie, Ph.D. thesis, Univ. of Bonn, Bonn, Germany, 1994.

Müller, M., A. Kraus, and A. Hofzumahaus, O_3 $O(^1D)$ photolysis frequencies determined from spectroradiometric measurements of solar actinic UV-radiation: Comparison with chemical actinometer measurements, *Geophys. Res. Lett.*, *22*, 679–689, 1995.

Parsons, T. R., M. Takahashi, and B. Hargrave, *Biological Oceanographic Processes*, 3rd ed., Pergamon, New York, 1984.

Peltzer, E. T., and P. G. Brewer, Some practical aspects of measuring DOC—Sampling artefacts and analytical problems with marine samples, *Mar. Chem.*, *41*, 243–253, 1993.

Plass, C., R. Koppmann, and J. Rudolph, Measurements of dissolved nonmethane hydrocarbons in sea water. *Fresenius J. Anal. Chem.*, *339*, 746–749, 1991.

Plass, C., R. Koppmann, and J. Rudolph, Light hydrocarbons in the surface water of the mid-Atlantic, *J. Atmos. Chem.*, *15*, 235–251, 1992.

Plass-Dülmer, C., A. Khedim, R. Koppmann, F. J. Johnen, J. Rudolph, and H. Kuosa, Emissions of light nonmethane hydrocarbons from the Atlantic into the atmosphere, *Global Biogeochem. Cycles*, *7*, 211–228, 1993.

Plass-Dülmer, C., R. Koppmann, M. Ratte, and J. Rudolph, Light nonmethane hydrocarbons in seawater, *Global Biogeochem. Cycles*, *9*, 79–100, 1995.

Ratte, M., C. Plass-Dulmer, R. Koppmann, J. Rudolph, and J. Denga, Production mechanism of C2–C4 hydrocarbons in seawater: Field measurements and experiments, *Global Biogeochem. Cycles*, *7*, 369–378, 1993.

Ratte, M., O. Bujok, A. Spitzy, and J. Rudolph, Laboratory experiments on the origin of C2–C3 alkenes in seawater, paper presented at the CACGP/IGAC Symposium, Comm. on Atmos. Chem. and Global Pollut., Fuji-Yoshida, Japan, Sept. 5–9, 1994.

Ratte, M., C. Plass-Dülmer, R. Koppmann, and J. Rudolph, Horizontal and vertical profiles of light hydrocarbons in sea water related to biological, chemical and physical parameters, *Tellus B*, *47*, 607–623, 1995.

Riemer, D. D., W. H. Pos, and R. G. Zika, Photochemical production of nonmethane hydrocarbons (NMHCs) in seawater: A process involving dissolved organic matter (DOM), *Eos Trans. AGU*, *77*(46), Fall Meet. Suppl., F256, 1996.

Röth, E. P., A fast algorithm to calculate the photonflux in optically dense media for use in photochemical models, *Ber. Bunsenges. Phys. Chem.*, *96*, 417–420, 1992.

Rudolph, J., and D. H. Ehhalt, Measurements of C2–C5 hydrocarbons over the North Atlantic, *J. Geophys. Res.*, *86*, 11,959–11,964, 1981.

Rudolph, J., F. J. Johnen, A. Khedim, and G. Pilwat, The use of automated "on line" gaschromatography for the monitoring of organic trace gases in the atmosphere at low levels, *Int. J. Environ Anal. Chem.*, *38*, 143–155, 1989.

Sachs, L., *Angewandte Statistik*, 7th ed., Springer-Verlag, New York, 1992.

Schobert, B., and E. F. Elstner, Production of hexanal and ethane by *Phaeodactylum tricornutum* and its correlation to fatty acid oxidation and bleaching of photosynthetic pigments, *Plant. Physiol.*, *66*, 215–219, 1980.

Thomas, C., G. Cauwet, and J. F. Minster, Dissolved organic carbon in the equatorial Atlantic Ocean, *Mar. Chem.*, *49*, 155–169, 1995.

Weiss, P. S., S. S. Andrews, J. E. Johnson, and O. C. Zafiriou, Photoproduction of carbonyl sulfide in South Pacific Ocean waters as a function of irradiation wavelength, *Geophys. Res. Lett.*, *22*, 215–218, 1995.

Wilson, D. F., J. W. Swinnerton, and R. A. Lamontagne, Production of carbon monoxide and gaseous hydrocarbons in seawater: Relation to dissolved organic carbon, *Science*, *168*, 1577–1579, 1970.

World Meteorological Organization (WMO), Atmospheric ozone 1985: Assessment of our understanding of the processes controlling its present distribution and change, *Rep. 16*, Global Ozone Res. and Monit. Proj., Geneva, 1985.

Zuo, Y., and R. D. Jones, Formation of carbon monoxide by photolysis of dissolved marine organic material and its significance in the carbon cycling of the oceans, *Naturwissenschaften*, *82*, 472–474, 1995.

O. Bujok, Institut für Stratospharische Chemie (ICG-1), Forschungszentrum Jülich, D-52425 Jülich, Germany.

M. Ratte, Institut für Atmosphärische Chemie (ICG-3), Forschungszentrum Julich, D-52425 Jülich, Germany. (e-mail: ratte@rwth-aachen.de)

J. Rudolph (corresponding author), Centre for Atmospheric Chemistry and Department of Chemistry, York University, North York, Ontario, Canada M3J 1P3.

A. Spitzy, Institut für Biogeochemie und Meereschemie, Universität Hamburg, Bundesstrasse 55, D-20146 Hamburg, Germany.

(Received June 10, 1997; revised November 5, 1997; accepted November 26, 1997.)